Digest Journal of Nanomaterials and Biostructures Vol. 7, No. 2, April - June 2012, p. 745 - 753

# EFFECT OF MnO SHELL TO PREVENT SINTERING OF FePt NANOPARTICLES DURING THE ANNEALING PROCESS

SEYED ALI SEBT, HOSSEIN ZEYNALI*, HADI ARABI[a],
HOSSEIN AKBARI, MOHAMMAD REZA HANTEH ZADEH
*Department of Physics, Science and Research Branch, Islamic Azad University, P. O. Box 14665-678, Tehran, Iran*
[a]*Magnetism and Superconducting Research Lab., Physics Department, University of Birjand, Birjand, Iran*

Monodispersed 4.1 nm FePt nanoparticles with narrow size distribution were successfully synthesized by the chemical polyol process with co-reduction of $Fe(acac)_3$ and $Pt(acac)_2$ in the presence of 1,2 hexadecanediol as a reducing agent and oleic acid and oleyl amine as a surfactant. To achieve $L1_0$ ordered structure, annealing at high temperature is required to realize phase transformation from face center cubic (fcc) to face center tetragonal (fct) phase. In this situation, FePt nanoparticles joining together and their size become larger than 20 nm. This is due to thermal decomposition of organic surfactant (oleic acid and oley amnie) at temperature around of 350 $^oC$. In the present work, we could to prevent sintering of FePt nanoparticles during the annealing process at temperatures of 650 and 750 $^oC$ by using the core/shell structure. In this case, MnO nanoparticles were used successfully as the shell around of each FePt core particles to protect them from sintering. As results, coercivity, Hc, of FePt and FePt/MnO nanoparticles after annealing at 650 $^oC$ is equal with 5 kOe and 2 kOe, respectively. With increasing annealing temperature to 750 $^oC$, the coercivity of these nanoparticle increases dramatically as value of 10 kOe and 5 kOe, respectively.

(Received March 5, 2012; Accepted June 1, 2012)

*Keywords:* Polyol process, co-reduction, FePt nanoparticles, Sintering, Core/shell, Phase transformation

## 1. Introduction

The $L1_0$ phase of FePt nanoparticles has high uniaxial magnetocrystalline anisotropy ($K_u$=6.6 $\times 10^7$ erg/cm$^3$), saturation magnetization of about 1140 emu/cm$^3$ and high energy products,$(BH)_{max}$, around of 13 MGOe [1-3], making it an excellent candidate in many applications, such as: (i) ultra-high magnetic recording media, (ii) high performance permanent magnets, (iii) sensors and drug carriers in biomedical [4-8].

To achieve ultra-high density magnetic recording media, it is limited to the single domain regime. So that the small particle sizes (bits) due to their single domain regimes can be leaded to increasing areal density. The minimum critical size for single domain FePt nanoparticles with $L1_0$ phase, which has thermal stability, is about 2.8 nm [9]. When the size of nanoparticles is less than a minimum critical size, magnetization of the particles becomes unstable and superparamagnetic behavior appears at room temperature, which is unsuitable for magnetic recording media applications. In the much literatures, FePt nanoparticles have been made successfully using

*Corresponding author : zeynali.ph@gmail.com

different chemically methods such as solution phase method [10], direct synthesis [11], and sol-gel [12].

The as-synthesized FePt nanoparticles by these methods have the chemically disordered face-centered cubic (fcc) structure, where the Fe and Pt atoms are distributed randomly in the crystal lattice and have superparamagnetic behavior at room temperature [13-15]. Annealing at the high temperatures (up to 550 $^{o}$C) is required for phase transformation of FePt nanoparticles from chemically disordered fcc structure to the chemically ordered fct structure with high uniaxial magnetocrystalline anisotropy. By the annealing process, organic surfactant (oleic acid and oleyl amine) start to decompose at a temperature above 350 $^{o}$C and due to that sintering of particles take place and particles size become larger than before. In order to prevent sintering of FePt nanoparticles different methods have been suggested. One of these methods is lowering the ordering temperature using the additive metal such as Ag [16], and Au [17]. Li et al [18], have shown that in his work, the salt method (NaCl) able to prevent sintering of nanoparticles. Also Yano et al [19], shown that rapid thermal annealing can be effective to prevent sintering of nanoparticles.

Core/shell structure is an interesting approach to prevent coalescence of magnetic nanoparticles where the magnetic cores were coated with Non-magnetic oxide shells, $SiO_2$ [20], and MgO [21] or magnetic shell $Fe_3O_4$ [22] and $CoFe_2O_4$ [23]. In the previous work, we were used the magnetic shell particles as $CoFe_2O_4$ to prevent coalescence of $Fe_{100-x}Pt_x$ particle. After annealing our results demonstrate that $CoFe_2O_4$ shell have impressive role to protect core particles from sintering, but the result is a low coercivity [24].

In the present work monodisperse FePt nanoparticles have been successfully synthesized by a polyol process in the presence of 1,2hexadecandiol and oleic acid and oleyl amines [25-29]. Then a shell of MnO nanoparticles around of FePt core particles have been created and annealing at temperature of 650 and 750 $^{o}$C for 2h under reducing atmosphere performed to phase transition take place from chemically disordered A1 to chemically ordered $L1_0$ phase. It seems that, MnO nanoparticles with a high melting temperature of 1650 $^{o}$C are able to protect FePt nanoparticles during the annealing process. Also MnO nanoparticles with Neel temperature of 122 $^{o}$K [30], have non-magnetic behavior at room temperature and do not have any interaction with the magnetic core particles. Results demonstrate that crystal structure and magnetic properties such as magnetization and coercivity can be changed by modification of annealing process.

## 2. Experimental

### 2.1. Synthesis of FePt core nanoparticles

Monodisperse FePt nanoparticles were synthesized by the co-reduction of $Fe(acac)_3$ (0.5 - mmol), $Pt(acac)_2$ (0.25 mmol), 1,2-hexadecanediol (2.5 mmol) in the presence of oleic acid (5 mmol), oleylamine (5 mmol) and 10 mL of benzyl ether under a flow of $N_2$ atmosphere. Mixing was performed for 20 min in order all powder completely dissolved and then reduction of Fe and Pt atoms in the presence of 1,2 hexadecanediol have been obtained and the nucleation of FePt starts to begin. Afterward, the mixture was heated to the boiling point of benzyl ether (300 $^{o}$C) with heating rate of 5 $^{o}$C in the presence of reflux and kept at this temperature for 15 min before cooling down to room temperature under a flow of $N_2$ atmosphere by removing the heat source.

Purification process of the black product was executed as following: 40 ml ethanol was added to the mixture and the black product was precipitated and separated via centrifugation (8000 rpm, 10 min). The ethanol impurities separated and black discarded was dispersed in hexane in the presence of oleic acid and oleyl amine. Centrifugation (8000 rpm, 10 min) was achieved again to remove any undispersed residue. Finally, the synthesized 4.1 nm FePt core are used as the seeds to produce FePt/MnO core/shell nanoparticles, which MnO shell nanoparticles were already synthesized by another polyol process.

### 2.2. Synthesis of MnO Shell Nanoparticles

The synthesis of MnO nanoparticles with shell thickness less than 1 nm, was achieved by the following procedure: $Mn(acac)_2$ (0.5 mmol), 1,2 hexadecanediol (5 mmol), oleic acid (1.5 mmol) and oleyl amine (1.5 mmol) are mixed together in 10 mL benzyl ether at room temperature under a flow of $N_2$ atmosphere. 10 mL hexane solution of as-synthesized 4.1 nm FePt nanoparticles was added to the reaction flask as the cores, and the content was magnetically stirred for 20 min under flow of $N_2$ atmosphere. Then the mixture was heated to the boiling point of benzyl ether (300 $^oC$) with heating rate of 5 $^oC$ in the presence of reflux and kept at this temperature for 15 min before cooling down to room temperature under a flow of $N_2$ atmosphere by removing the heat source.

The black products were centrifuged following the procedure described in the synthesis of 4.1 nm FePt core nanoparticles. Finally, FePt/MnO core/shell nanoparticles were obtained after a series of centrifugation.

### 2.3. Nanoparticles Characterization

The structure, morphology and magnetic properties of samples (prepared FePt and FePt/MnO nanoparticles) were investigated by some equipped analytical systems. Samples for transmission electron microscopy (TEM) analysis were prepared by evaporating a hexane solution of dispersed particles on amorphous carbon coated copper grids. The size of core and core/shell nanoparticles was determined using a JEM-2100 model working at 200 kV. ImageJ software has been used to calculate the histogram and average size of FePt nanoparticles. For calculation the average size of FePt nanoparticles, using this software, all the particles in TEM images have been considered. X-ray powder diffraction, STOE diffractometer with Cu-Kα source (λ=1.5405 $A^o$), was used for studying the crystallinity of FePt and FePt/MnO nanoparticles. The magnetization measurements were carried out using a vibrating sample magnetometer (Lake Shore 7400) with the maximum field up to 20 kOe. The FePt and FePt/MnO nanoparticles were annealed under a reducing atmosphere (%93Ar+%7$H_2$) using conventional quartz tube furnace at 650 and 750 $^oC$ for 2h.

## 3. Result and discussion

Figure 1a shows the TEM image of as-synthesized FePt nanoparticles which have spherical shapes and well isolated, which made at the first step. Figure 1b is the histogram of FePt nanoparticles size distribution based on log-normal fitting. Histogram graph shows that the particles have a single size with an average diameter (<d>) about 4.1 nm and standard deviation (σ) of about 0.36 nm, indicate narrow size distribution (σ/<d>) of 0.09.

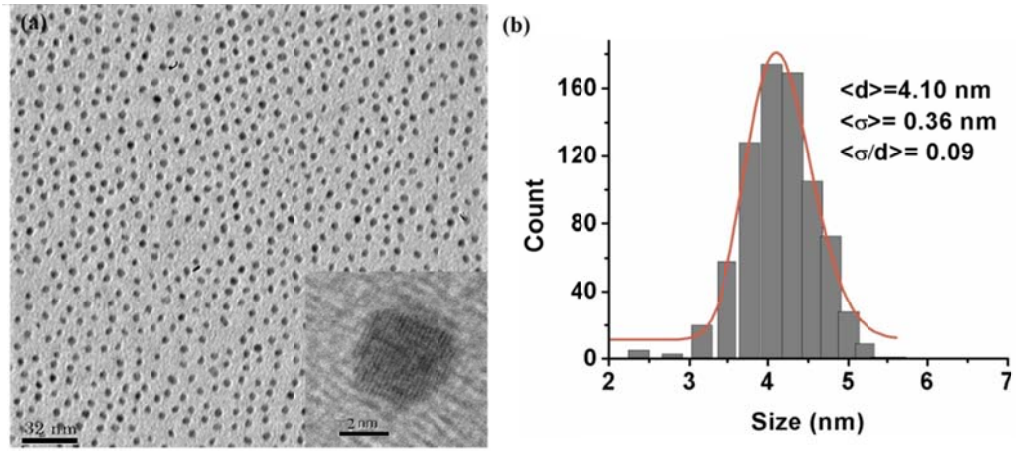


*Fig. 1. (a) TEM image and (b) Histogram of as-synthesized FePt nanoparticles with the size of 4.1 nm.*

Fig. 2 shows the TEM images of as-synthesized FePt/MnO core/shell nanoparticles which have also spherical shapes and well isolated. Due to synthesis process, the middle parts of nanoparticles are darker show FePt core, and around of these nanoparticles is brighter shows MnO shell thickness. The distinct contrast between the core and shell region is due to the difference in electron penetration efficiency at the metallic FePt core particles and MnO oxide shell. The analyses of HRTEM with different magnification indicate that the shell thicknesses are less than 1 nm in the Figure 2c and 2d, respectively.

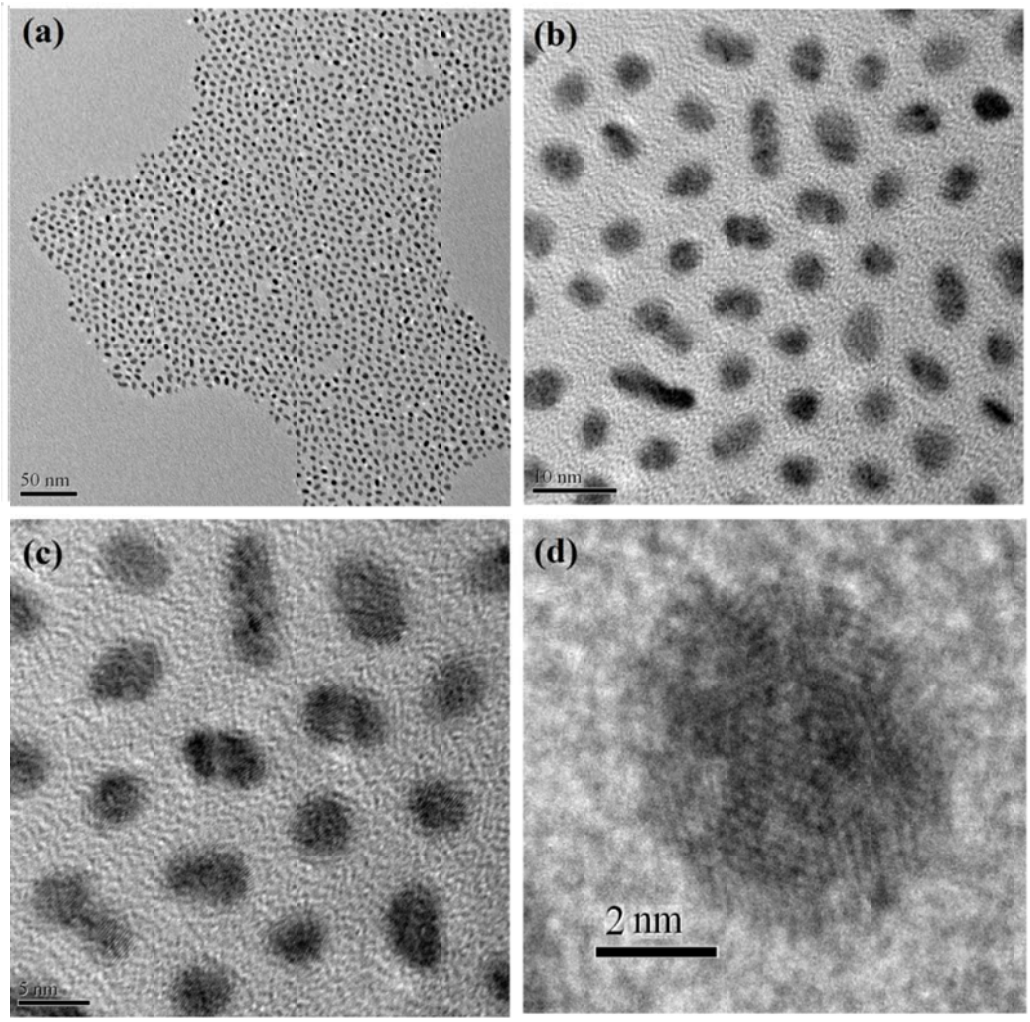


*Fig. 2. (a) - (d) TEM and HRTEM image with different magnification of as-synthesized FePt / MnO core/shell nanoparticles.*

Figure 3 shows the X-ray diffraction patterns (XRD) of as-synthesized FePt and FePt/MnO nanoparticles. The (111), (200) and (220) peaks of FePt structure represents disordered fcc structure in the both as-synthesized core and core/shell samples. An average diameter of as-synthesized FePt nanoparticles was calculated from the peak broadness of the (111) by Using Scherrer equation [31], and it is about 4.2 nm that is in agreement with TEM results. Moreover the (111) peak at $2\theta = 34.40^{o}$ and (220) at $2\theta = 59.50^{o}$ is related to the MnO structure (Figure 3b).

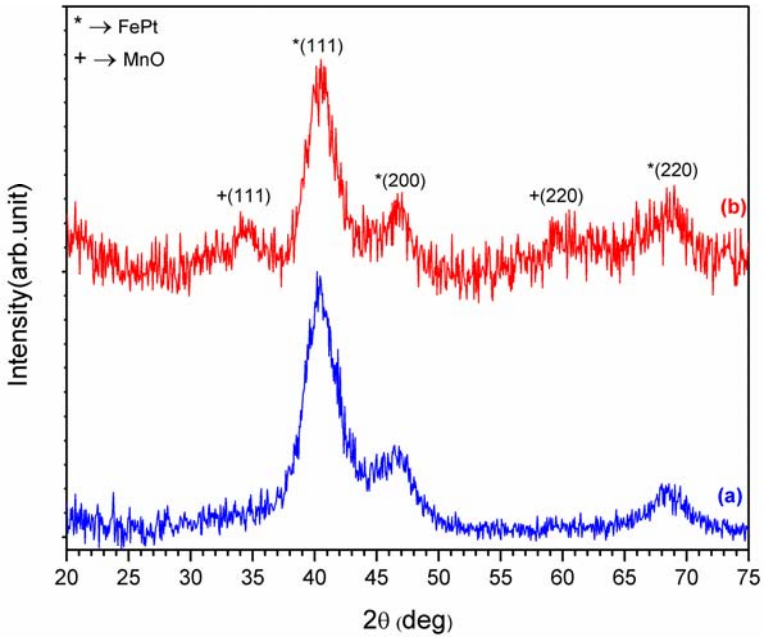


*Fig. 3. (a) and (b) are XRD patterns of as-synthesized FePt and FePt/MnO nanoparticles, respectively.*

Figure 4 shows the XRD pattern of annealed FePt and FePt/MnO core/shell nanoparticles. Figure 4a and 4c associated to the FePt nanoparticles which are annealed at 650 and 750 $^{o}$C, respectively and Figure 4b and 4d related to FePt/MnO nanoparticles at the same temperature, respectively. Annealing at 650 $^{o}$C for 2 h under a reducing atmosphere (%93Ar + %7 $H_2$) leads to transformation for disordered FePt nanoparticles occurred to chemically ordered $L1_0$ phase (Figure 4a).

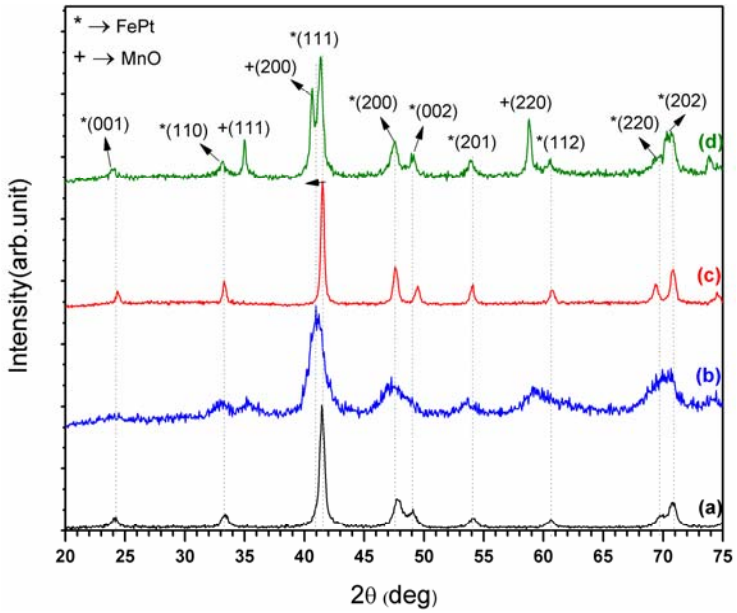


*Fig. 4. (a) and (b) are XRD pattern of annealed FePt and FePt/MnO nanopartices at temperature of 650 $^{o}$C.*

Characteristic (001) peak at 24.06$^{o}$ definitely belonging to the $L1_0$ structure of FePt and the other peaks for $L1_0$ phase of fct structure are: (110) at $2\theta$=33.30$^{o}$, (111) at 41.47$^{o}$, (200) at 47.87$^{o}$, (002) at 49.02$^{o}$ and (220) at 69.78$^{o}$ and (202) at 70.74$^{o}$. In the case of FePt/MnO nanoparticles, annealing at 650 $^{o}$C for 2 h leads to partial ordering in $L1_0$ phase, which is clear from the XRD patterns (Figure 4b). There is quite differences between two structure of FePt and

FePt/MnO nanoparticles. The (200) peak is a characteristic feature peak which identified the difference between $L1_0$ phase of FePt and FePt/MnO at 650 $^oC$. For the annealed FePt/MnO, this peak placed at $2\theta=47.36^o$, while in the case of FePt $L1_0$ phase, this peak split into (200) and (002) tetragonal peaks, similarly, this phenomenon happened for the (220) peak of FePt/MnO, which is split into (220) and (202) peaks in XRD patterns of FePt $L1_0$ phase.

The same structural behavior happened for FePt and FePt/MnO nanoparticles when the particles were annealed at 750 $^oC$ for 2 h. In this case chemical ordering can be seen as the narrowing of XRD peaks, suggesting an improvement in atomic ordering of Fe and Pt than the other one at 650 $^oC$. Further confirmation occurs by appearance of clearly (001) and (110) ordered peaks at 24.30 and $33.30^o$, respectively. Also tetragonal peaks of (200)/(002) and (220) /(202) showing up completely and spilt each other confirming an improvement in atomic ordering (Figure 4c-4d). In the case of FePt/MnO nanoparticles, XRD patterns have two series of peaks. One set is related to the chemically ordered $L1_0$ peaks and the other peaks of MnO oxide shell.

The existence of oxide shell around each particle has an effect on the crystal structure of FePt. By annealing of FePt/MnO nanoparticles at 650 $^oC$, the diffraction pattern shows weak oxide peaks at $35.25^o$, which corresponds to the (111) diffraction peak of MnO, which are more developed by increasing the annealing temperature to 750 $^oC$ and also found that another peaks of MnO structure in the XRD patterns at $40.60^o$ and $58.77^o$ corresponding to the (200) and (220) peaks, respectively. The narrow peak at $41.47^o$ in the Fig. 4a and 4c ensures that the particles in these samples are joined together and sintering of particles is occurred. These results will be interesting more, when have comparative studies on the Figure 4a with 4b with Figure 4c with 4d. Appearing the broad peaks for FePt/MnO (Figure 4b and 4d) at $2\theta=41.30^o$ rather than narrow peaks for FePt (Figure 4a and 4c) confirms that the MnO shell can effectively prevent coalescence of nanoparticles. Furthermore, there is a noticeable shift of the (111) peak to lower angle for FePt/MnO nanoparticles, suggesting the partial degree of ordering of $L1_0$ phase with fct structure.

TEM analyses of annealed particles (core and core/shell) have been compared in the Figure 5 at temperature of 750 $^oC$.

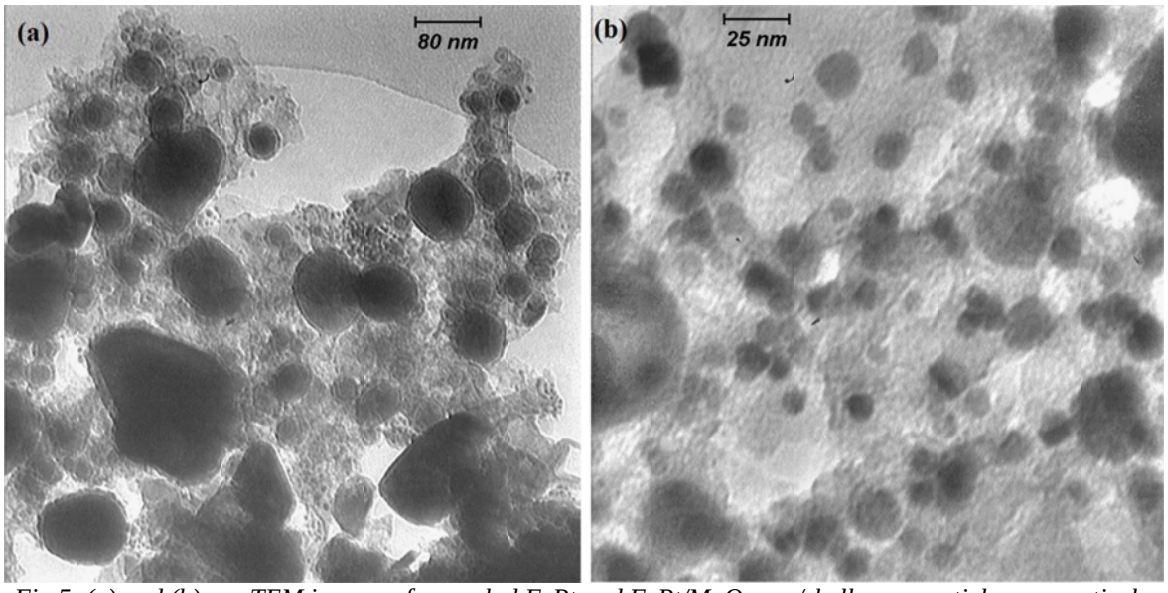


*Fig.5. (a) and (b) are TEM images of annealed FePt and FePt/MnO core/shell nanoparticles, respectively.*

Clearly, in the case of FePt core particles (Figure 5a), annealing at 750 $^oC$ for 2 h leads to large agglomeration (average sizes are more than 20 nm), while for FePt/MnO core/shell particles (Figure 5b) annealing at the same conditions reveals partial coalescence. The size of coalesced particles in the core/shell structure is in the range of 7-10 nm, which confirms that the MnO oxide shell can effectively prevent coalescence of the nanosized core particles.

Figure 6 shows the hysteresis loops of as-synthesized FePt and FePt/MnO nanoparticles at room temperature.

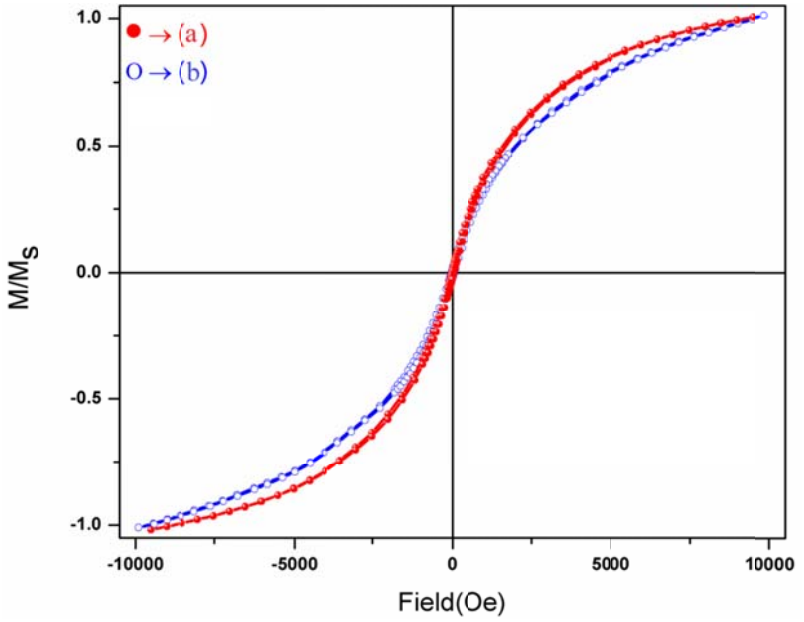


*Fig 6. Hysteresis loops of as-synthesized nanoparticles (a) FePt (b) FePt/MnO*

The as-synthesized FePt nanoparticles have chemically disordered fcc structure and are superparamagnetic at room temperature due to their low magnetic anisotropy. Since, MnO nanoparticles are non-magnetic at room temperature; there was no interaction between the FePt core and MnO shell particles and therefore as-synthesized FePt/MnO core/shell particles considered as a superparamagnetic at room temperature.

Figure 7 shows the hysteresis loops of FePt and FePt/MnO nanoparticles after annealing at 650 and 750 $^{O}$C. As can be seen from Figure 7a, coercivity, Hc, of FePt and FePt/MnO nanoparticles after annealing at 650 $^{o}$C is equal with 5 kOe and 2 kOe, respectively. With increasing annealing temperature, the coercivity of these nanoparticle increases dramatically. So that, after annealing at 750 $^{o}$C, coercivity of FePt and FePt/MnO nanoparticles is equal with 10 kOe and 5 kOe, respectively (Figure 7b).

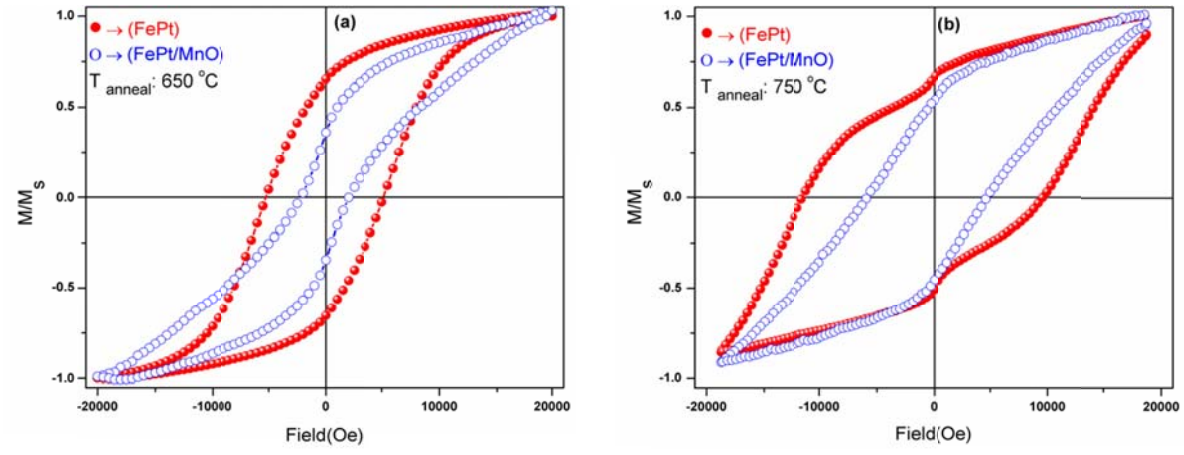


*Fig. 7. Hysteresis loops of annealed FePt and FePt/MnO nanopartices at temperature of (a) 650 $^{o}$C (b) 750 $^{o}$C.*

Appearing high coercivity after annealing similar the results of XRD, indicating the improvement of $L1_0$ ordering at 750 $^{o}$C rather than 650 $^{o}$C. Such magnetic behavior, difference of coercivity after annealing, can be explained by coherent rotation model (Stoner-Wohlfarth Model) [32]. Using the Stoner-Wohlfarth model, it is clear that with increasing particle size, magnetocrystalline uniaxial anisotropy energy increases, which means that the magnetic field required to overcome the anisotropy energy, can be increased and resulting that the coercivity will

be increased. So considering that the average size of core nanoparticles in the FePt structure after annealing at both temperatures (650 and 750 $^{o}$C) is larger than the average size of same core nanoparticles in the FePt/MnO core/shell structure, hence it can be concluded that the coercivity of FePt nanoparticles is higher than the coercivity of FePt/MnO nanoparticles.

## 4. Conclusion

The as-synthesized FePt nanoparticles have chemically disordered fcc structure and are superparamagnetic at room temperature due to their low magnetic anisotropy. Annealing at the temperature above 550 $^{o}$C leads to transformation of disordered A1 phase occurred to the ordered $L1_0$ phase. During annealing process, the organic surfactant (oleic acid and oleyl amine) around each particle start to decompose and sintering of the nanoparticles occurs and large agglomeration is formed. We in this work at the first step attempt to synthesized monodisperse 4.1 nm FePt nanoparticle by chemical polyol process and at the next step we try to prevent sintering of FePt nanoparticles under annealing process by adding of MnO oxide shell around of each core particles. It observed the MnO shell particles are able to protect FePt nanoparticles from sintering at annealing temperature of 750 $^{o}$C. As the result, coercivity for FePt nanoparticles with $L1_0$ phase is about 10 kOe, while it's about 5 kOe for FePt/MnO nanoparticle with $L1_0$ phase.

**Acknowledgments**

This work was supported by the Physics Research Center, Science & Research Branch at Islamic Azad University and the Magnetic & Superconducting Research Lab at Birjand University. The authors thank North-Eastern Hill University, Shillong-793022, India (http://www.nehu.ac.in/Services/SAIF) for transmission electron microscopy analysis of core/shell nanoparticles.

## References

[1] F. T Yuan, H.W. Chang, K. L. You, Y. Liou, T. S. Chin, C. C. Yu, Y. D. Yao, Nanotechnology. **18,** 33560 (2007).
[2] H. Zenga, S. Sun, T. S. Vedantam, J. P. Liu, Z. R. Dai, and Z. L. Wang, APPLIED PHYSICS LETTERS. **80**, 2583-2585(2002).
[3] D. C. Lee, F. V. Mikulec, J. M. Pelaez, B. Koo, and B. A. Korgel, J. Phys. Chem. B. **110**, 11160-11166 (2006).
[4] V. Nandwana, K. E. Elkins, N. Poudyal, G. S. Chaubey, K. Yano, and J. P. Liu, J. Phys. Chem. C. **111**, 4185-4189 (2007).
[5] S. Sun, S. Anders, T. Thomson, J. E. E. Baglin, M. F. Toney, H. F. Hamann, C. B. Murray, and B. D. Terris, J. Phys. Chem. B. **107**, 5419-5425 (2003).
[6] C. B. Rong, N. Poudyal, and J. P. Liu, J. Phys. D: Appl. Phys. **43,** 495001(2010).
[7] H. G. Bagaria, D. T. Johnsona, C. Srivastava, G. B. Thompson, M. Shamsuzzoha, and D. E. Nikles, JOURNAL OF APPLIED PHYSICS. **101**, 104313 (2007).
[8] M. Nakaya, M. Kanehara, and T. Teranishi, Langmuir. **22**, 3485-3487 (2006).
[9] S. Sun, E. E. Fullerton, D. Weller, and C. B. Murray, IEEE TRANSACTIONS ON MAGNETICS. **37**, 1239-1243 (2001).
[10] S. Sun, C.B. Murray, D. Weller, L. Folks, and A. Moser, Science. **287**, 1989 (2001).
[11] M.S. Wellons, W.H. Morris, Z. Gai, J. Shen, J. Bently, J.E. Witting, and C.M. Lukehart, Chem. Mater. **19**, 2483(2007).
[12] N. Shukla, J. Ahner, and D. Weller, J. Magn. Magn. Mater. **E1349**, 272-276 (2004).
[13] C. B. Rong, , V. Nandwana, N. Poudyal, G. S. Chaubey, and J. P. Liu, IEEE TRANSACTIONS ON NANOTECHNOLOGY. **8**, 437-443 (2009).
[14] M. Mito, Y. Komorida, N. J. O. Silva, H. Tsuruda, H. Deguchi, S. Takagi, T. Tajiri, T. Iwamoto, and Y. Kitamoto, JOURNAL OF APPLIED PHYSICS. **108**, 124315 (2010).

[15] T. Iwamoto, Y. Kitamoto, and N. Toshima, Physica B. **404**, 2080-2085 (2009).
[16] S. Kang, J. W. Harrell, and D. E. Nikles, Nano Lett. **2**, 1033-1036 (2002).
[17] Z. Jia, S. Kang, S. Shi, D. E. Nikles, and J. W. Harrell, JOURNAL OF APPLIED PHYSICS. **97**, 10J310 (2005).
[18] D. Li, N. Poudyal, V. Nandwana, Z. Jin, K. Elkins, and J. P. Liu, JOURNAL OF APPLIED PHYSICS. **99**, 08E911 (2006).
[19] K. Yano, V. Nandwana, N. Poudyal, C. B. Rong, and J. P. Liu, JOURNAL OF APPLIED PHYSICS. **104**, 013918 (2008).
[20] Y. Tamada, S. Yamamoto, M. Takano, S. Nasu, and T. Ono, APPLIED PHYSICS LETTERS. **90**, 162509 (2007).
[21] J. Kim, C. Rong, J. P. Liu, and S. Sun, Adv. Mater. **21**, 906–909 (2009).
[22] L. C. Varand, M. Imaizumi, F. J. Santos, and M. Jafelicci, IEEE TRANSACTIONS ON MAGNETICS. **44**, 4448-4451 (2008).
[23] G. S. Chaubey, V. Nandwana, N. Poudyal, C. B. Rong, and J. P. Liu, Chem. Mater. **20**, 475-478 (2008).
[24] H. Akbari, S. A. Sebt, H. Arabi, H. Zeynali, and M. Elahi, Chemical Physics Letters. **524**,78-83(2012).
[25] K. E. Elkins, T. S. Vedantam, J. P. Liu, H. Zeng, S. Sun,Y. Ding and Z. L. Wang, Nano Lett. **3**, (2003).
[26] C. Liu, X. Wu, T. Klemmer, N. Shukla, X. Yang , D. Weller ,A. G. Roy, M. Tanase, D. Laughlin, J. Phys. Chem. B. **108**, 6121-6123(2004).
[27] L. C. Varanda, and M. Jafelicci, J. AM. CHEM. SOC. **128**, 11062-11066 (2006).
[28] C.Liu, X. Wu, T. Klemmer, N. Shukla, and D. Weller, Chem. Mater. **17**, 620-625 (2005).
[29] V. Nandwana, K. E. Elkins and J. P. Liu, Nanotechnology. **16**, 2823–2826 (2005).
[30] M. Ghosh, K. Biswas, A. Sundaresana, and C. N. R. Rao, J. Mater. Chem. **16**, 106–111 (2006).
[31] B.E. Warren, X-Ray Diffraction, Dover Publications, New York, (1990).
[32] B. D. Cullity, and C. D. Graham, INTRODUCTION TO MAGNETIC MATERIALS, Second Edition , AJOHN WILEY & SONS, INC. PUBLICATION (2009).